We are IntechOpen, the world's leading publisher of Open Access books Built by scientists, for scientists

4,800
Open access books available

122,000
International authors and editors

135M
Downloads

Our authors are among the

154
Countries delivered to

TOP 1%
most cited scientists

12.2%
Contributors from top 500 universities

CLARIVATE ANALYTICS BOOK CITATION INDEX INDEXED

WEB OF SCIENCE™

Selection of our books indexed in the Book Citation Index in Web of Science™ Core Collection (BKCI)

Interested in publishing with us?
Contact book.department@intechopen.com

Numbers displayed above are based on latest data collected.
For more information visit www.intechopen.com

10

Cellular Automaton Modeling of Passenger Transport Systems

Akiyasu Tomoeda
Meiji Institute for Advanced Study of Mathematical Sciences, JST CREST,
Meiji University,
1-1-1 Higashi Mita, Tama-ku, Kawasaki, Kanagawa,
Japan

1. Introduction

Jamming phenomena are observed everywhere in our daily live. These stagnations in flow occur not only on highways, but also in stadiums, in public transportation like buses and trains, in the world of the Internet, and even in our bodies. Almost everyone will have a negative image of a "jam", which means the clogging of the flow of traffic, however we do have positive reactions to some kinds of jams. For instance, it is gratifying to interrupt the transmission of infectious disease or prevent the spreading of fire.

The important point is that all these kinds of phenomena have the commonality of being a congestion in a transporting process which comes about through a universal jamming formation process. Especially from the point of statistical physics, these jamming phenomena are also interesting as a system of interacting particles, such as vehicles, pedestrians, ants, Internet packets, and so on, driven far from equilibrium. By considering all the above particles in various transporting processes as "Self-Driven Particles" (SDPs), we are allowed to treat various transportation phenomena universally under the physics of complex systems [1–3] . This interdisciplinary research on jamming phenomena of SDPs in various fields has been recently termed as "Jamology" [4, 5] .

Now, let us consider the state of "Jam", i.e., what is a "Jamming flow"? It is difficult for anyone to answer this question exactly. Japanese expressway companies incorporate specific threshold velocities to define the jamming flow. That is, if the average traffic velocity becomes less than the defined threshold velocity, the state of traffic is considered to have transitioned to a jamming flow. Whereas, if the average traffic velocity is above the threshold, the state of traffic flow corresponds to "Free flow". For example, one company defines the threshold velocity to be 40km per hour. In this case, if the average traffic velocity becomes less than 40km per hour, the state of traffic flow is called jamming flow. Whereas, another company identifies jamming flow by defining the threshold as 30km per hour. There is a lack of uniformity, since the definition of jamming flow depends on the company. Moreover, when it comes to considering the jamming phenomena in the dynamics of non-vehicles, such as pedestrians and ants, it becomes difficult to properly translate these definitions based on threshold velocity to another definition of the jamming state in the dynamics of non-vehicles. Thus, we should begin to provide a clear definition of jamming flow in the next section to study jamming phenomena as a mathematical science.

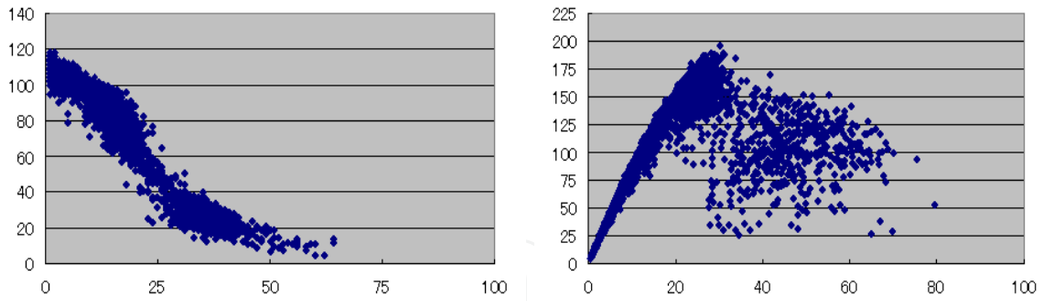

(a) density vs. velocity (b) density vs. flow

Fig. 1. Fundamental diagrams plotted by real data from a Japanese expressway (one-lane data). The horizontal axis indicates the density of vehicles (vehicles/km) and the vertical axis indicates (a) the velocity (km/hour) and (b) flow (vehicles/hour), respectively.

First, in Sec. 2 of this chapter, we introduce the *fundamental diagram* to provide a clear definition of jamming flow and explain two rule-based models for describing the dynamics of SDPs, the so-called *Asymmetric Simple Exclusion Process* (ASEP) and *Zero Range Process* (ZRP), which can capture fundamental features of jamming phenomena in various collective dynamical systems. These models have the important property of being exactly solvable, that is, their steady states are given by a form [6–11] . Therefore, we treat the behavior of particles in complex systems by not only numerical simulations but also analytical calculations in the steady state. In Sec. 3, as an extension of the above stochastic cellular automata, we explain in detail the *Public Conveyance Model* (PCM) [12] , which is a fundamental mathematical model for the passenger transport system by introducing a second field (passengers field) which tracks the number of waiting passengers. In addition, by introducing the route choice model of passengers explicitly into PCM, we have built a real-time railway network simulation tool "KUTTY", which has been applied to the *Tokyo Metro Railway Network* [13, 14] , as described in Sec. 4. Finally, Sec. 5 is devoted to concluding discussions.

The aim of this chapter is to understand the mathematical model for the passenger transport system built on analytical rule-based models and to introduce the real-time railway network simulation tool "KUTTY" as an application of our proposed model.

2. Fundamental diagrams and stochastic cellular automata

Now we introduce the *fundamental diagram* to provide a clear definition of jamming flow. The fundamental diagram is a basic tool in understanding the behavior of the flow in transportation systems: it relates the flow $Q(x,t)$ in the system and the density of vehicles $\rho(x,t)$ [1] . The fundamental is sometimes drawn to indicate the relation between velocity $v(x,t)$ and density $\rho(x,t)$, however, we can easily translate velocity into flow by the relation $Q = \rho v$.

Fig. 1 is an example of the fundamental diagrams of a Japanese expressway. From these diagrams, it is obvious that the state of traffic flow and velocity strongly depend on the density

[1] In the following, we use *"particle"* in mathematical models to represent a vehicle, a bus, or a train, to keep this discussion as general as possible.

of vehicles on the road. So long as the density is sufficiently small, the average velocity is practically independent of the density as the vehicles are too far apart to interact. Therefore, at sufficiently low density of vehicles, the system effectively acts in a state of "free flow". However, in practice, vehicles have to move more slowly with increasing density. This reality is correctly described in the fundamental diagrams.

As mentioned before, each expressway company in Japan defines the jamming state by a threshold velocity. Hence, there is no universal definition of the jamming state that can be treated in a mathematical sense. In order to provide a clear definition of "free flow" and "jamming flow", one transforms the vertically plotted value from velocity to flow, i.e., from Fig. 1 (a) to Fig. 1 (b). Surprisingly, this type of fundamental diagram (Fig. 1 (b)) shows the universal features not only in the dynamics of traffic vehicles but also for other general SDPs as follows (also see Fig. 2):

(a) At low density, there is almost a linear relation between the flow and the density, which intersects at zero. The slope at low density corresponds to the average velocity without congestion.

(b) If the density exceeds some critical value, the so-called *critical density* ρ^c, the flow decreases monotonically and it vanishes together with the velocity at some maximum density. [2]

(c) The flow has one maximum value at medium density.

The critical density indicates the changing point of the flow state from free flow to jamming flow. Therefore, free flow and jamming flow can be defined as the lower density region and higher density region which are separated by the critical density as shown in Fig. 2. Once free flow and jamming flow are defined in terms of the fundamental diagram, one can determine whether the flow is really in a state of "Jam" or not in a rigorous, mathematical sense, even in the dynamics of various other kinds of SDPs, where the jamming state has been considered undefinable or unclear. Thus, the fundamental diagrams are essential to treat the jamming phenomena as a mathematical science.

Now let us introduce two simple stochastic cellular automaton models, i.e., ASEP and ZRP, which are the simple models for non-equilibrium systems of interacting self-driven particles. In these cellular automaton models, the path (a road or rail) is partitioned into L identical cells such that each cell can accommodate at most one particle at a time, enforcing the so-called *exclusion principle*, that is, the excluded-volume effect is not supposed to be ignored unlike in the flow of water. [3] Generally, the dynamics of these models are described by a rule [4]. The rule for dynamics of particles in case of ASEP is very simple, i.e., "*If the front cell is empty, a particle can move forward with hopping probability p.*" as shown in Fig. 3. Note that, in general,

[2] In several situations involving vehicle dynamics, it has been observed that flow does not depend uniquely on density in an intermediate regime of density. This indicates the existence of a *hysteresis effect* and *metastable states*. The critical density in vehicle dynamics is about 25 (vehicles/km).

[3] In traditional queuing theory, this excluded-volume effect and spatial structure have never been introduced into the queuing model. An extension of the $M/M/1$ queuing process with a spatial structure and excluded-volume effect is introduced in [15, 16] , as the TASEP on a semi-infinite chain with open boundary.

[4] Some of them can be described in the form of equations, such as a "master equation" or "max-plus equation / tropical-polynomial".

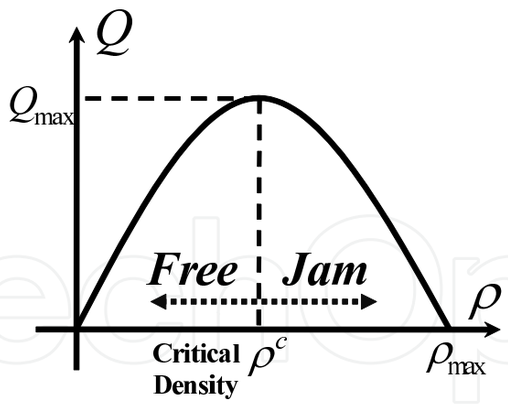

Fig. 2. Features and definition of the jamming state in the simplified fundamental diagram (density vs. flow).

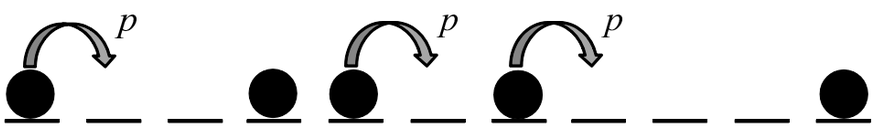

Fig. 3. Dynamics of the Asymmetric Simple Exclusion Process: if the next cell is empty, a particle can move forward with hopping probability p.

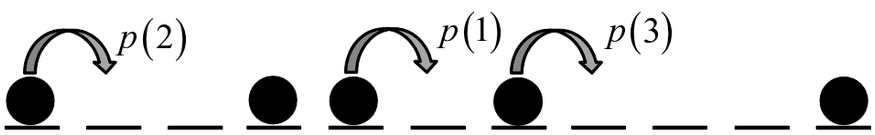

Fig. 4. Dynamics of the Zero Range Process after the mapping to the asymmetric exclusion process: if the next cell is empty, a particle can move forward with hopping probability $p(h)$, which depends on the distance to the next particle in front.

ASEP is characterized by the hopping rate

$$P_{\{10\}\to\{01\}} = p, \tag{1}$$

$$P_{\{01\}\to\{10\}} = q, \tag{2}$$

which is considered as a model of interacting random walks.

The most important special case, theoretically as well as in the application to transport systems, is known by the full name of *Totally Asymmetric Simple Exclusion Process* (TASEP), which has $q = 0$ so that its motion is allowed only in one direction. Here, we use the general name ASEP to mean TASEP for simplicity' sake. Moreover, the hopping probability p is usually called the hopping rate in ASEP, since time is continuous in ASEP. However, we call the rate p the hopping probability p, since we treat only the discrete time case in this chapter.

In the case of ZRP, after a suitably precise mapping, the rule is considered as "*If the front cell is empty, a particle can move forward with hopping probability $p(h)$, which depends on the distance to*

the next particle in front.", as illustrated in Fig. 4. Indeed, ASEP is considered as a special case of ZRP.

Here, we impose periodic boundary conditions [5] , that is, we consider that the particles to move on a circuit so that the transport system is operated as a loop. This means that the number of particles N on the circuit is conserved at each discrete time step. Moreover, we distinguish three basic types of dynamics: the dynamical variables may be updated one after the other in a certain order (*sequential update*), one after another in random order (*random-sequential update*), or in parallel for all sites (*parallel update*). [6] Now let us employ the parallel update for all sites in the system as the updating procedures.

As mentioned before, ASEP and ZRP have the important property of being exactly solvable, that is, their steady states are given by a form [6–11] . In the case of ASEP with periodic boundary condition and in parallel dynamics, one obtains the form (see [7] for details)

$$Q(\rho) = \frac{1}{2}\Big[1 - \sqrt{1 - 4p\rho(1-\rho)}\Big], \tag{3}$$

where $Q(\rho)$ is flow of particles, p is the hopping probability and $\rho = N/L$ is the density of particles.

On the other hand, in the case of ZRP, as a simple example, we now assume that the hopping probability is

$$p(1) = p, \quad p(h \geq 2) = q. \tag{4}$$

If $q = p$, this model is reduced to the ASEP with hopping probability p, as denoted above. Moreover, if $p = q = 1$ in ZRP or $p = 1$ in ASEP, this model is reduced to the deterministic version of ASEP, which is called the rule-184 cellular automaton. This rule-184 CA model is one of the elementary cellular automata, which are defined by S. Wolfram (1959 $\sim$) [17, 18] . Various extensions of this rule-184 CA are also proposed as a powerful model for realistically describing one-dimensional traffic flow.

The fundamental diagram of ZRP defined by (4) with periodic boundary conditions and parallel update in a parametric representation, where the density $\rho(w) = 1/(1+h)$ and the flow $Q(\rho) = w\rho(w)$ are calculated for the parameter $0 \leq w \leq 1$, is given by the following equations (see [11] for details)

$$F(w) = \Big(1 - p(1)\Big)(1+w)\sum_{n=0}^{\infty}\Big(w^n \prod_{j=1}^{n}\frac{1-p(j)}{p(j)}\Big), \tag{5}$$

$$h(w) = w\frac{\partial}{\partial w}\Big(\log F(w)\Big). \tag{6}$$

Fig. 5 shows the numerical simulation results (dots) and analytical calculated results (line) for ASEP and ZRP, respectively. In both cases, the analytical results show good agreements with the numerical results. Moreover, both figures captures the universal features $(a) - (c)$ of general SDPs in transport systems, which were introduced earlier in this section. Therefore,

[5] ASEP and ZRP with open boundary conditions are also well investigated.

[6] Sometimes, updating the dynamics in parallel for all sites of a given sub-lattice (*sub-lattice update*) is distinguished from this parallel update.

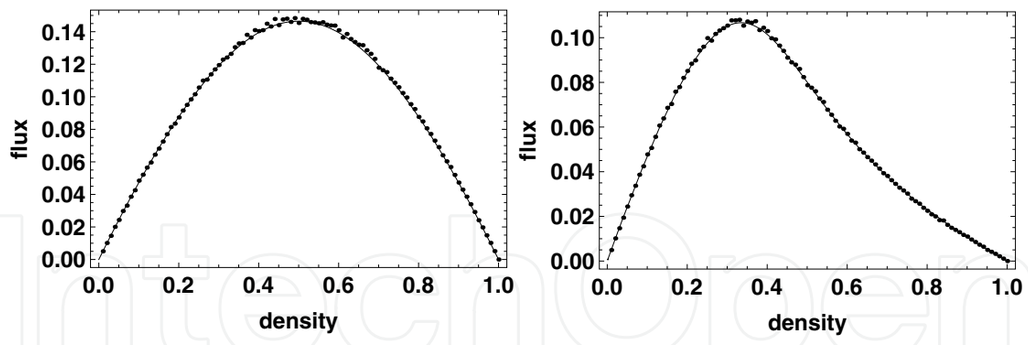

(a) ASEP (b) ZRP

Fig. 5. Fundamental diagram of (a) Asymmetric Simple Exclusion Process and (b) Zero Range Process with the parallel update. The dots and the line correspond to the simulation data and analytical results, respectively. The numerical simulations are done with $L = 100$ sites. In the case of ASEP, the hopping probability p is 0.5. In the case of ZRP, the hopping probability $p(h)$ is $p(0) = 0, p(1) = 0.1, p(2 \geq h) = 0.5$.

various extensions of these models have been reported in the last few years for capturing the essential features of the collective spatio-temporal organizations in wide varieties of systems, including those in vehicular traffic [1, 2, 19] .

Until now, public conveyance traffic systems such as buses, bicycles and trains have also been modeled by an extension of ASEP using similar approaches [12–14, 20, 21]. A simple bus route model [21] exhibits clustering of the buses along the route. The quantitative features of the coarsening of the clusters have strong similarities with coarsening phenomena in many other physical systems. Under normal circumstances, such clustering of buses is undesirable in any real bus route as the efficiency of the transportation system is adversely affected by clustering.

In the next section, a new public conveyance model (PCM) will be explained which is applicable to buses and trains in a transport system by introducing realistic effects encountered in the field (the number of stops (stations) and the behavior of passengers getting on a vehicle at stops) into the stochastic cellular automaton models.

3. Public conveyance model for a bus-route system

Now we will explain the PCM in detail. Although we refer to each of the public vehicles as a "bus", which is a one-dimensional example of a transport system, the model is equally applicable to train traffic on a given route. We impose periodic boundary conditions as well as the stochastic cellular automata described in the previous section and partition the road into L identical cells. Moreover, a total of S ($0 \leq S \leq L$) *equispaced* cells are identified in the beginning as bus stops. Note that, the special case $S = L$ corresponds to the *hail-and-ride* system, in which the passengers could board the bus whenever and wherever they stopped a bus by raising their hand. In contrast to most of the earlier bus route models built on the stochastic cellular automaton, we assume that the maximum number of passengers that can get into one bus at a bus stop is $N_{\max}$, which indicates the *maximum boarding capacity* at each bus stop rather than the *maximum carrying capacity* of each bus.

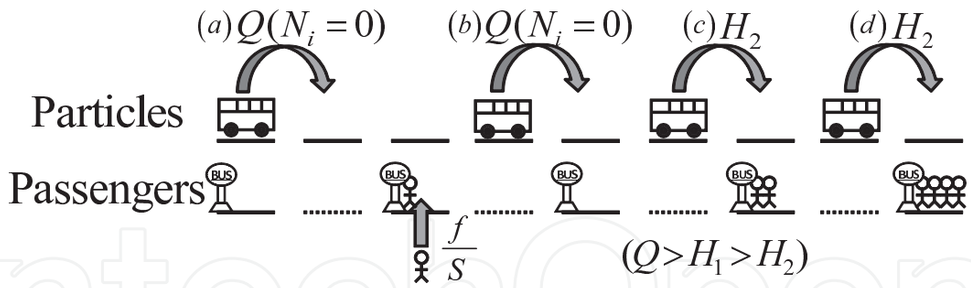

Fig. 6. Schematic illustration of the PCM. The hopping probability to the bus stop depends on the number of waiting passengers. Accordingly, if the waiting passengers increase, the hopping probability to the bus stop decreases. Although case (a) and (b) is the same hopping probability, the situation is different: (a) next cell is without bus stop, (b) next cell is with bus stop but without passengers. Case (d) has smaller probability than the case (c), since the hopping probability depend on the number of waiting passengers. Of course, case (c) is smaller than the case (b) (also case (a))).

The symbol H is used to denote the hopping probability of a bus entering into a cell that has been designated as a bus stop. We assume H has the form

$$H = \frac{Q}{\min(N_i, N_{\max}) + 1} \tag{7}$$

where $\min(N_i, N_{\max})$ is the number of passengers who can get into a bus which arrives at the bus stop i at the instant of time when the number of passengers waiting at the bus stop i $(i = 1, \cdots, S)$ is N_i. The form (7) is motivated by the common expectation that the time needed for the passengers to board a bus is proportional to their number. Fig. 6 depicts the hopping probabilities schematically. The hopping probability of a bus to the cells that are not designated as bus stops is Q; this is already captured by the expression (7) since no passenger ever waits at those locations.

If the form H does not depend on the number of waiting passengers but depends on the presence of passengers in the case $S = L$, i.e.,

$$H = \begin{cases} Q & \text{no waiting passengers,} \\ q & \text{waiting passengers exist,} \end{cases} \tag{8}$$

where both Q and q $(Q > q)$ are constants independent of the number of waiting passengers, this model corresponds to the *Ant-Trail-Model*, which also shows quite similar clustering phenomena to those of vehicles in the collective movement of ants and obtains the results through approximate analysis [22, 23] . Moreover, if the form H is always constant, this model is reduced to the ASEP.

In principle, the hopping probability H for a real bus would depend also on the number of passengers who get off at the bus stop; in the extreme situations where no passenger is waiting at a bus stop, the hopping probability H would be solely decided by the disembarking passengers. However, in order to keep the model theoretically simple and tractable, we ignore the latter situation and assume that passengers get off only at those stops where waiting passengers get into the bus and that the time taken by the waiting passengers to get into the bus is always adequate for the disembarking passengers to get off the bus.

The PCM model reported here can be easily extended to incorporate an additional dynamical variable associated with each bus to account for the instantaneous number of passengers in it. But, for the sake of simplicity, such an extension of PCM is not reported here [7] . Instead, we focus on the simple version of PCM. As shown in Fig. 7, the model is updated according to the following rules:

1. *Arrival of a passenger*
   A bus stop i ($i = 1, \cdots, S$) is picked up randomly, with probability $1/S$, and then the corresponding number of waiting passengers is increased by unity, i.e., $N_i \to N_i + 1$, with probability f to account for the arrival of a passenger at the selected bus stop. Thus, the average number of passengers that arrive at each bus stop per unit time is given by f/S.
2. *Bus motion*
   If the cell in front of a bus is not occupied by another bus, each bus hops to the next cell with probability H. Specifically, if passengers do not exist in the next cell the hopping probability equals Q because N_i is equal to 0. Otherwise, if passengers exist in the next cell, the hopping probability is $Q/(\min(N_i, N_{\max}) + 1)$. Note that, when a bus is loaded with passengers to its maximum boarding capacity $N_{\max}$, the hopping probability is $Q/(N_{\max} + 1)$, the smallest allowed hopping probability.
3. *Boarding a bus*
   When a bus arrives at the i-th ($i = 1, \cdots, S$) bus stop cell, the corresponding number N_i of waiting passengers is updated to $\max(N_i - N_{\max}, 0)$ to account for the passengers boarding the bus. Once the door is closed, no more waiting passengers can get into the bus at the same bus stop although the bus may remain stranded at the same stop for a longer period of time either because of the unavailability of the next bus stop or because of the traffic control rule explained next.

We introduce a traffic control system that exploits the information on the number of buses in each *segment* between successive bus stops, as well as a block section of the railway system. Every bus stop has information I_i ($i = 1, \cdots, S$) which is the number of buses in the i-th segment of the route between the i-th and next $(i+1)$-th bus stops at that instant of time. If I_i is larger than the average value $I_0 = m/S$, where m indicates the total number of buses, a bus remains stranded at a stop i as long as I_i exceeds I_0. In steps 2, 3, and the information-based control system (step 4), these rules are applied in parallel to all buses and passengers, respectively.

We use the average speed $\langle V \rangle$ of the buses, the number of waiting passengers $\langle N \rangle$ at a bus stop and the transportation volume R, which is defined by the product of velocity of the i-th bus $V_i \in \{0, 1\}$ and the number of on-board passengers M_i ($0 \le M_i \le N_{\max}$), i.e.,

$$R = \sum_{i=1}^{m} M_i V_i, \tag{9}$$

as three quantitative measures of the efficiency of the public conveyance system under consideration; a higher $\langle V \rangle$, a higher R and smaller $\langle N \rangle$ correspond to a more efficient transportation system.

[7] We have reported the extended PCM by incorporating the disembarking passengers explicitly for the case of the elevator system in [24] .

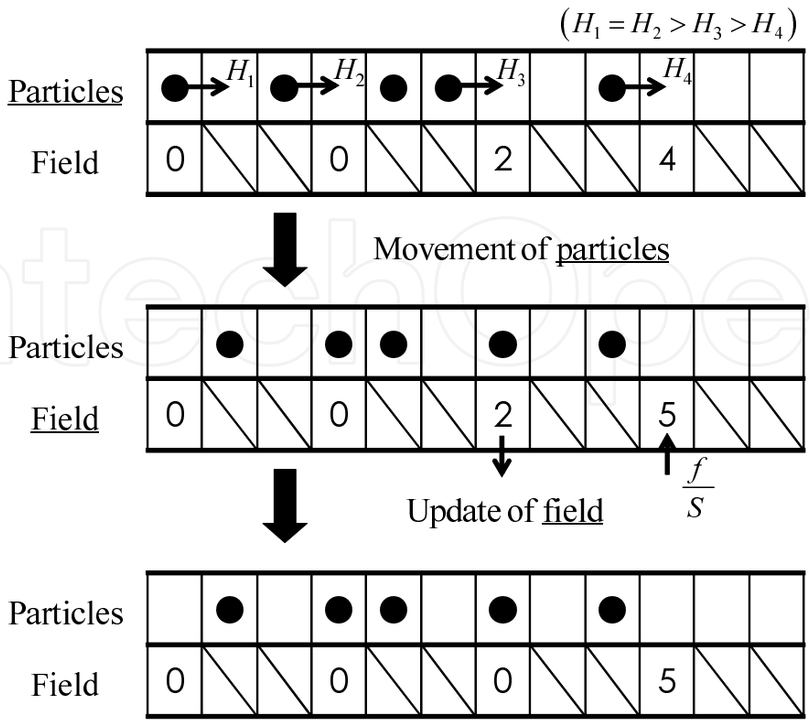

Fig. 7. Time development of public conveyance model. The upper path of cells indicates the state of particles and the lower one indicates the state of passengers. The number in each cell represents the number of waiting passengers. The cells with diagonal lines indicate cells without bus stops.

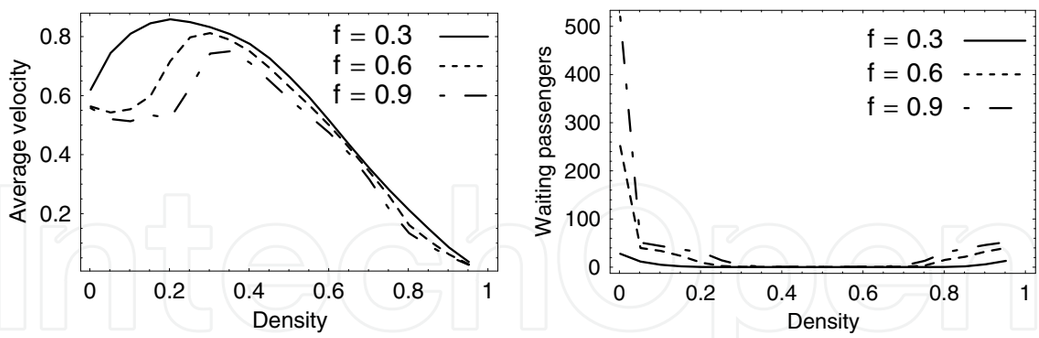

(a) Average velocity $\langle V \rangle$ (b) Waiting passengers $\langle N \rangle$

Fig. 8. The plot of $\langle V \rangle$ and $\langle N \rangle$ without information for $S = 5$ and $f = 0.3$, 0.6 and 0.9.

In the simulations presented here, we set $L = 500, S = 5, Q = 0.9, q = 0.5$ and $N_{\max} = 60$. The main parameters of this model, which we varied, are the number of buses m and the probability f of the arrival of passengers. The density of buses is defined by $\rho = m/L$ in the same way. We study not only the efficiency of the system but also the effects of our control system by comparing the characteristics of two traffic systems one of which includes the information-based control system while the other does not.

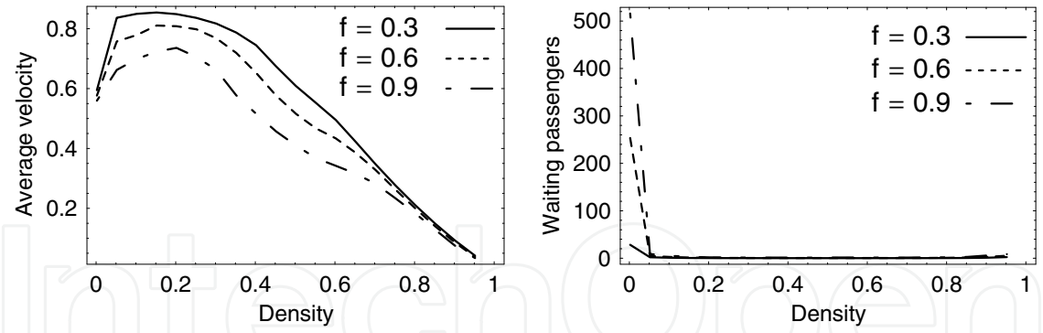

(a) Average velocity $\langle V \rangle$ (b) Waiting passengers $\langle N \rangle$

Fig. 9. The plot of $\langle V \rangle$ and $\langle N \rangle$ with information for $S = 5$ and $f = 0.3$, 0.6 and 0.9

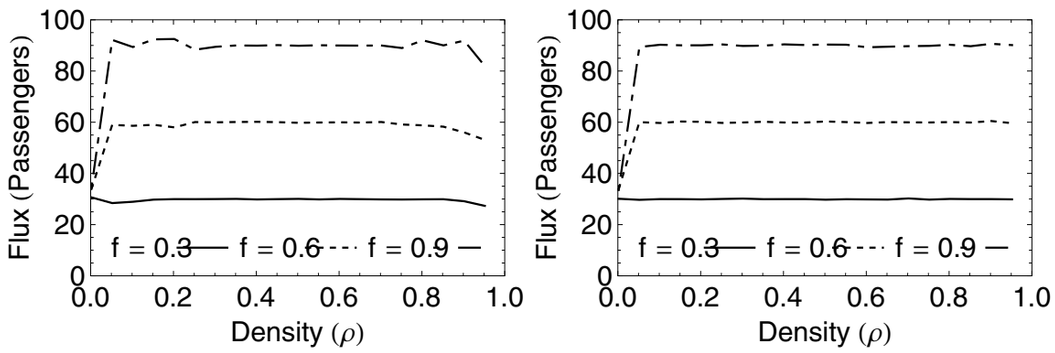

(a) without information (b) with information

Fig. 10. Fundamental diagrams for the transportation volume. (a) The case without the information-based control system, (b) The case with the information-based control system.

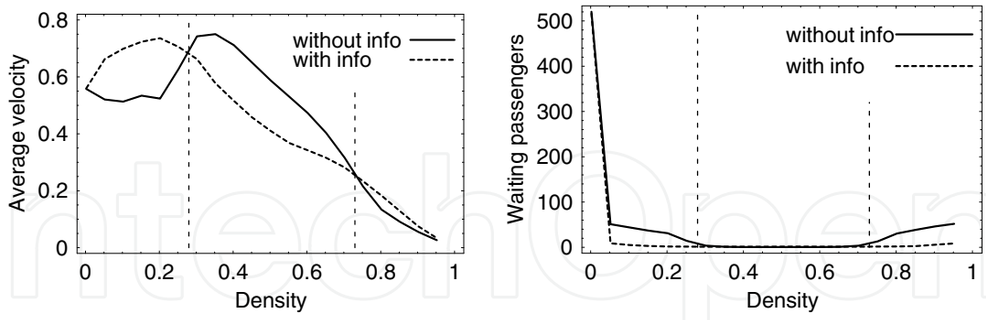

(a) Average velocity $\langle V \rangle$ (b) Waiting passengers $\langle N \rangle$

Fig. 11. Two efficiency plots $\langle V \rangle$ and $\langle N \rangle$ for the parameters $S = 5, Q = 0.9, q = 0.5$, and $f = 0.9$.

Some of the significant results of the numerical simulations of the PCM are as follows. In Fig. 8 and Fig. 9, we plot $\langle V \rangle$ and $\langle N \rangle$ against the density of buses for several different values of f. Fig. 8 (a) demonstrates that the average speed $\langle V \rangle$, which is a measure of the efficiency of the bus traffic system, exhibits a *maximum* at around $\rho = 0.2 \sim 0.3$, which reflects the bus bunching especially at large f. As shown in Fig. 8 (b), The average number of waiting

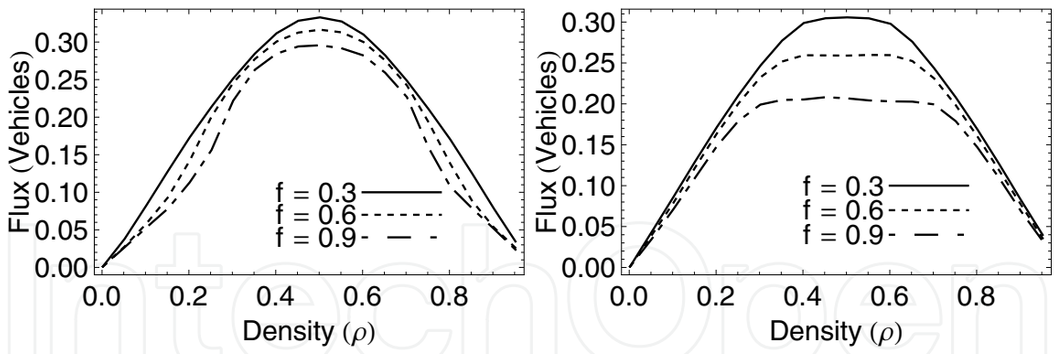

(a) without information (b) with information

Fig. 12. Fundamental diagrams for the flow of vehicles. (a) The case without the information-based control system, (b) The case with the information-based control system.

passengers $\langle N \rangle$, whose inverse is another measure of the efficiency of the bus traffic system, is vanishingly small in the region $0.3 < \rho < 0.7$; $\langle N \rangle$ increases with decreasing (increasing) ρ in the regime $\rho < 0.3$ ($\rho > 0.7$). The results for the PCM with information-based traffic control system are shown in Fig. 9. The density corresponding to the peak of the average velocity shifts to lower values when the information-based traffic control system is switched on. The average number of waiting passengers $\langle N \rangle$ decreases between Fig. 8 (b) and Fig. 9 (b) in the regions $0.1 < \rho < 0.3$ and $0.7 < \rho < 0.9$.

The other measurement of the efficiency, the transportation volume R, is shown in Fig. 10. The optimal density which shows higher $\langle V \rangle$ and lower $\langle N \rangle$ does not always correspond to the most efficient operation for the transportation volume, since that is maintained substantially constant except at low density, even though the density of vehicles increases. This is because the number of buses with small transportation volume increases even though the average velocity decreases. Thus, we have found that the excess buses result in unneeded buses which has no passengers since the transportation volume is the same.

The data shown in Fig. 11 establishes that implementation of the information-based traffic control system does not necessarily always improve the efficiency of the public conveyance system. In fact, in the region $0.3 < \rho < 0.7$, the average velocity of the buses is higher if the information-based control system is switched off. Comparing $\langle V \rangle$ and $\langle N \rangle$ in Fig. 11, we find that the information-based traffic control system can improves the efficiency by reducing the crowd of waiting passengers. However, in the absence of waiting passengers, introduction of the information-based control system adversely affects the efficiency of the public conveyance system by holding up the buses at bus stops when the number of buses in the next segment of the route exceeds I_0. Therefore, we have found the information-based traffic control system can improve the efficiency in a certain density region, but not in all possible situations.

The typical fundamental diagrams for the flow of vehicles in the PCM are given in Fig. 12. The flow of vehicles without the information-based control system gradually decreases as the arrival rate of passengers increases. In contrast, the flow with the information-based control system drastically decreases for intermediate densities, where there are no waiting passengers in Fig. 9, showing a trapezoidal shape. This trapezoidal shape is similar to the fundamental diagram in [25] and [26] , where a blockage effect is artificially introduced into the rule-184 cellular automaton to take a flow bottleneck into account. Thus, in the absence of waiting

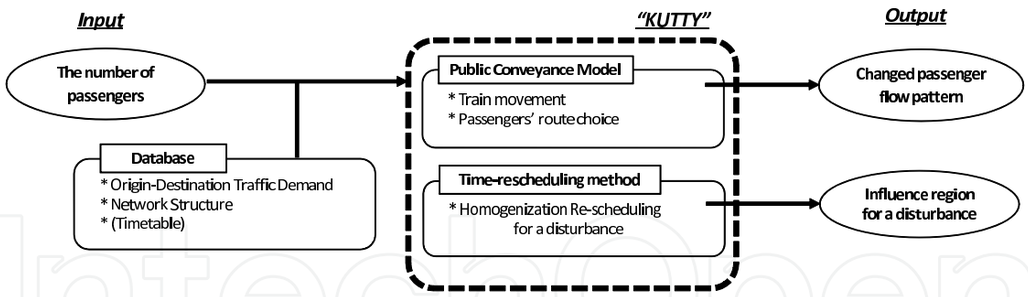

Fig. 13. The design flow diagram of our simulator "KUTTY".

passengers, implementation of the information-based control system corresponds to creating a bottleneck effect and decreases the flow of vehicles.

As a theoretical approach, mean-field analysis is also applied to the model to estimate the efficiency. The details of mean-field analysis can be found in [12–14] .

Next, let us explain an expanded PCM for the railway transportation system in the Tokyo metropolitan area by introducing the route choice model of passengers.

4. Public conveyance model for Tokyo metro subway network

Disturbances of well scheduled trains occur everyday. The disturbances may be caused by, for example, a slight delay of trains, traffic accidents, or other factors. Under such circumstances, how does the train company adjust and operate the train schedule? The conventional method of rescheduling the timetable is that the scheduling specialists adjust the timetable by their own empirical rules. This conventional method usually only considers the performance of a single (metro) line and does not take into account the performance of the whole network. Furthermore, this method tries to adjust the trains so that they are equally-spaced in time without considering the flow of passengers. Recently, various kinds of models of the train network, which treat the network as a complex system, have been proposed and studied [27–30]. However, the behaviors of passengers have not been considered in these models either.

A public conveyance model (PCM) which could reproduce the bus clustering phenomenon and estimate the efficiency of the bus system on a one-dimensional route was proposed in the previous section, where passengers arrive at a stop randomly and their destinations have not been considered explicitly. Furthermore, since buses run on a single route, passengers do not need to choose the route. In this section, we have extended the PCM by introducing realistic passengers' behaviors explicitly and proposed a real-time railway network simulation tool "KUTTY", which has been applied to the *Tokyo Metro Railway Network*. It is shown that the passenger flow pattern is well simulated. Moreover, we have presented a homogenization re-scheduling method to alleviate congestion of crowded trains, and it is found that our method is more efficient than the conventional one.

4.1 Database

Our real-time simulator "KUTTY" is operated not only based on the input data but also by extracting data from a database (see Fig. 13). In this section, we present the assembly of

the database and explain its components: *OD (origin-destination) traffic demand* and *network structure*.

4.1.1 Origin-destination traffic demand estimation

In order to apply our PCM to the railway transportation system in a realistic way, real data of the OD traffic demand of passengers is indispensable on the network. In general, it is very difficult to obtain this sort of data. Fortunately, the Tokyo Metro Company posts one-day rider-ship of all stations on its web-site. Moreover, at the mutual entry stations [8], the rider-ship also includes the influx and outflux of passengers. Nevertheless, the data only record the sum of passengers getting through the station gate and do not distinguish whether the passengers enter or leave the station. Therefore, we assume that half of the passengers enter the station and the other half leave the station. This is reasonable because most people go to work or school in the morning and go back home in the evening. Thus they return to the station where they originally entered .

Under these reasonable assumptions, we can estimate the OD demand from one-day rider-ship data of all stations and have verified that the estimated number of passengers is suitable for the data.

When a passenger enters a station i, the probability that the passenger's destination is j is

$$P_{i \to j} = \frac{N_j}{\sum_j N_j}, \tag{10}$$

where N_j indicates the number of passengers who leave from station j.

4.1.2 Network structure

In 2007, the Tokyo Metro Railway Network consisted of 8 lines and 138 stations [9] . Some of these stations are transfer stations, in which several lines intersect. In our model, the stations are mapped to nodes. Under our scheme, each node corresponds one-to-one to the ID number of each station on each line. That is, a transfer station is mapped to more than one nodes, depending on how many lines intersect (e.g., "Otemachi" of the Tozai Line (T09) and "Otemachi" of the Marunouchi Line (M18) are mapped to different nodes). The connection between neighboring stations is referred to as a "segment" and the connection inside a transfer station is referred to as a "link". Using this system, the Tokyo Metro Railway Network has 169 nodes, 170 segments and 50 links. Passengers can travel from any station to any other station in this network with at most two transfers. Therefore, the calculation time in searching for a possible route notably is decreased by restricting transfers to more than two. We have made the database of all paths by using *Dijkstra's Algorithm* [31].

4.2 Models and homogenization method

In this section, we first present the route choice model of the passengers. Then, the train movement model, which is built on PCM, is introduced. After that, we propose a homogenization re-scheduling method to alleviate congestion.

[8] The trains still move on from these stations, beyond which the transportation system is operated by other companies, such as Japan Railway. The mutual entry stations are shared by several companies.

[9] Since 2008, a new line has opened to traffic, but we have not included the new line here.

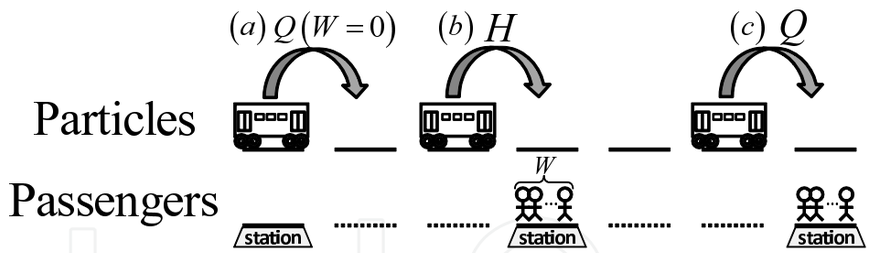

Fig. 14. Illustration of all cases of the hopping probability from a train: (a) Hopping into a non-platform cell. (b) Hopping into a platform cell (first time). (c) Hopping into a platform cell after one stop in the case of (b).

4.2.1 Route choice model

When a passenger p arrives at a station, his/her destination is determined by (10). Suppose $S(p)$ is the set of all routes from the origin to the destination. The cost E of each route $s \in S(p)$ at time t is calculated by

$$E\Big(T(p,s), C(p,s), D(p,s,t)\Big) = aT(p,s)^{\alpha} + bC(p,s)^{\beta} - cD(p,s,t)^{-\gamma}, \tag{11}$$

where $a, b, c, \alpha, \beta, \gamma$ are parameters with positive value. In this formula, $T(p,s)$ is the expected travel time on route s, $0 \leq C(p,s) \leq 2$ is the transfer number on route s. $T(p,s)$ is calculated by $T(p,s) = nT_t + C(p,s)T_c$. Here n is the number of stations on the route (excluding the origin) and T_t is set to 2 minutes, which denotes the average travel time between two neighboring stations. T_c is the average transfer time, which is set to 1 minute. The term $bC(p,s)^{\beta}$ is adopted to reflect how passengers are reluctant to transfer. Sometimes, passengers would rather choose a route with smaller $C(p,s)$, despite the fact that the travel time on this route is longer. $D(p,s,t)$ is defined as $D(p,s,t) = \max(D_{tr}, D_{pl})$, where $D_{tr} = \max_{i \in I}(D_{tr,i})$ and $D_{pl} = \max_{j \in J}(D_{pl,j})$. Here $D_{tr,i}$ is passenger density on train i at time t, and $D_{pl,j}$ is passenger density on platform j at time t; I denotes the set of all trains that move on route s at time t; J denotes the set of all platforms on route s.

The normalized probability $P(p,s,t)$, for the passenger p to select route s, is described as follows,

$$P(p,s,t) = \frac{\exp\Big[-E(p,s,t)\Big]}{\sum_{s_i \in S(p)} \exp\Big[-E(p,s_i,t)\Big]}. \tag{12}$$

This means that the smaller the cost $E(p,s,t)$ is, the larger is the probability that the route will be selected.

4.2.2 Train movement model

For simplicity, we assume that each *segment* of all lines is partitioned into four identical cells and each *platform* is designated as one cell such that each cell can also accommodate at most one train at a time. Fig. 14 depicts the hopping probabilities in the train model schematically. Let us denote the probability that trains hop into a non-platform cell as Q, the hopping probability of a train to a platform cell as H, the number of passengers waiting at the platform

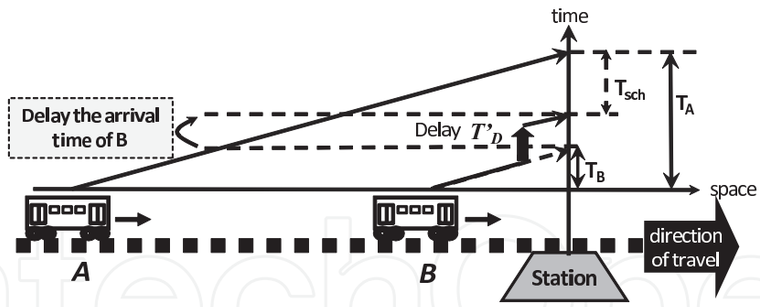

(a) One of the traditional methods

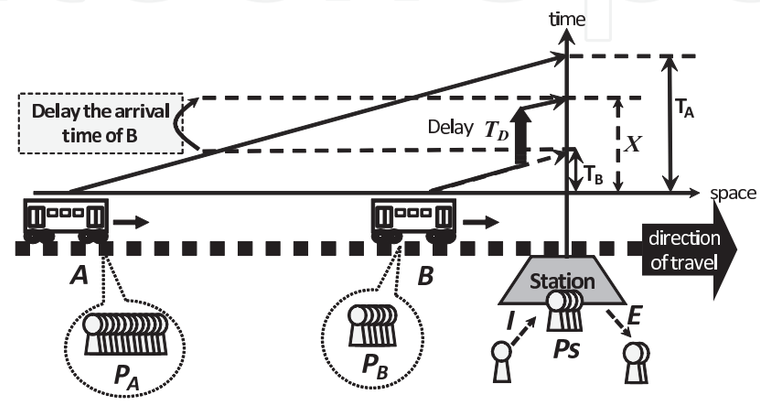

(b) Our homogenization method

Fig. 15. Two types of the re-scheduling methods. The traditional rescheduling method (a) is to adjust the time gap to T_{sch}. However, our homogenization method (b) is to adjust the time gap to a value which depends on the distribution of the number of passengers.

at the instant of time when a train arrives at the upstream neighboring cell as W and the maximum carrying capacity of trains as $W_{\max}$, we assume that

$$H = \min\left(\frac{1}{a' \min(W, W_{\max}) + 1}, Q\right), \tag{13}$$

where a' is a parameter. However, if the train fails to hop into the platform cell once, then it will hop with probability Q in the next time step. This is because trains are controlled in units of very small segment by the railway signaling system, and it is not realistic that trains stop stochastically again and again. In this section, the parameters are set to $a' = 0.2$, $Q = 1$.

4.2.3 Homogenization re-scheduling

Now let us propose a homogenization re-scheduling method. Suppose there is a sudden increase in passengers at a station. Since there are a lot of passengers waiting on the platform, the nearest upstream train from the station will become congested and thus delayed. If there is no re-scheduling, this train will become more and more delayed at the next stations.

In order to solve this problem, some re-scheduling method could be adopted by delaying the preceding trains of the delayed train, so that the congestion could be shared by preceding

trains. In the conventional re-scheduling method, this is fulfilled by equalizing the time gaps between neighboring trains. For instance (see Fig. 15), suppose that train B is expected to arrive at the next station at time $t = T_B$ and train A is expected to arrive at the station at time $t = T_A$. If $T_A - T_B > T_{sch}$, then the delay time of train B is determined by $T'_D = T_A - T_B - T_{sch}$ (see Fig. 15 (a)). Here T_{sch} is the scheduled time gap.

The delay times of trains located further downstream can be calculated similarly.

In our homogenization re-scheduling method, the number of passengers in each train is homogeneously-distributed by adjusting the distribution of trains as shown in Fig. 15 (b). Here P_B and P_A correspond to the number of boarding passengers on trains B and A respectively. P_s denotes the number of passengers waiting at the platform. E_B and E_A denote the number of passengers that will get off at the station i. Let symbol I be the number of passengers who arrive at the station per unit time. The expected arrival times of B and A at the station i are still denoted as T_B and T_A. Our objective is not equalizing the time gap but homogenizing the number of passengers, that is, the number of passengers on B and A is homogenized by extending T_B to X. We calculate X from the equation [10]

$$P_B + (P_s + IX) - E_B = P_A + I(T_A - X) - E_A. \tag{14}$$

The left-hand side (right-hand side) of (14) is the number of passengers on B (A) after departing from the station. The delay time T_D of B is thus decided by

$$T_D = X - T_B. \tag{15}$$

Having obtained the delay time of train B, the delay times of trains located further downstream can be calculated similarly.

4.3 Simulations and results

Fig. 16 shows two snapshots of our simulator "KUTTY" which display the direct simulation model and the flow pattern of the passengers of each segment as a visualization on the route map.

By simulating the flow of passengers quantitatively in all segments all over the network, we have found that the most congested area in the Tokyo Metro Railway Network is Otemachi Station on the Tozai Line (T09). Based on this result, we have simulated the case where a virtual accident occurs at Otemachi Station on the Tozai Line so that the trains of Tozai Line could only be operated on two sides of the station. Under this circumstance, the flow pattern of passengers will be changed significantly. This simulation, therefore, provides a very important clue for train scheduling with respect to the potential needs of users for alternative routes in case of accidents.

Fig. 17 shows the quantitative results of several simulations. Fig. 17 (a) shows that the number of passengers who take the Tozai Line decreasing by about 25 percent from normal operation due to the accident at T09. In contrast, the number of passengers who take the Ginza Line and the Hibiya Line increases by about 15 percent and 10 percent respectively. We believe this is

[10] Here we would like to mention that Eq.(5) is not always valid. For example, when $P_B + P_s - E_B > W_{\max}$, Eq.(5) will be invalid. In order for Eq.(5) to be valid, the conditions $T_B < X < T_A$ and $0 < P_B + (P_s + IX) - E_B < W_{\max}$ should be met. Fortunately, in our simulations, this is always the case.

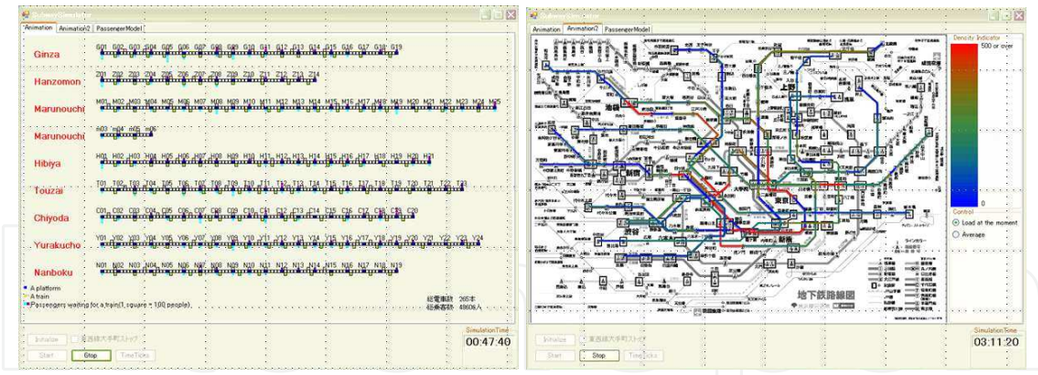

(a) Dynamical animation window (b) Visualization window

Fig. 16. Snapshots of our simulator "KUTTY". (a) The dynamical animation window of our model. (b) The entire map view, used to visualize the changing-flow in the route map. In KUTTY, the high flow regions (low-flow regions) are colored red (blue). This flow dynamically changes with time.

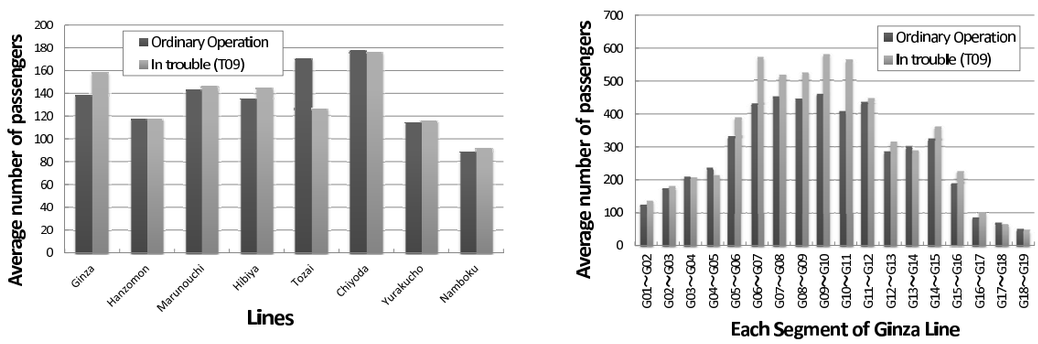

(a) per train in each line (b) per segment of the Ginza Line

Fig. 17. Comparison plot of the number of passengers between normal operation and operation with an accident at T09. (a)The number of passengers in each line comparing ordinary operation and congested conditions. (b)The number of passengers in each segment of the Ginza Line comparing ordinary operation and congested conditions.

because the Ginza Line intersects with the Tozai Line at T10, and the Hibiya Line intersects with the Tozai Line at T11, both of which are important transfer stations. In contrast, the Hanzomon Line intersects with the Tozai Line at T07, which is not such an important transfer station as T10 and T11. As a result, the passenger flow of the Hanzomon Line is essentially unaffected. Moreover, this result also implies that Otemachi Station is not the destination of most passengers on the Tozai Line, because otherwise the flow rate of the Hanzomon Line would increase (from T10 to Z09 to Z08, and from T07 to Z07 to Z08). Fig. 17 (b) shows the number of passengers on all segments of the Ginza Line. It can be seen that in the area from G05 to G11, the number of passengers increases remarkably. By transferring at these stations, passengers could change to the Marunouchi Line at G09, the Chiyoda Line at G06, and the Namboku Line at G05 and G06. Note that under normal operation, passengers change to the

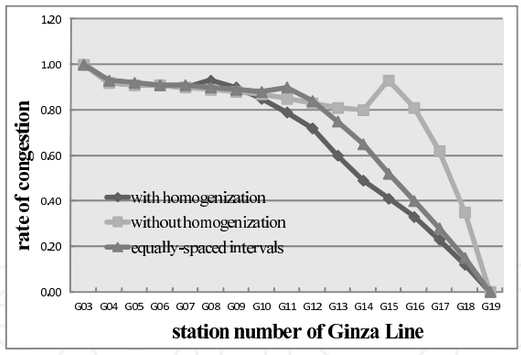

Fig. 18. Comparison plot of the passenger density of train A among the three systems. The congestion rate among the uncontrolled system, ordinary controlled system, and our homogenization system.

Marunouchi Line and to the Chiyoda Line at Station T09 and to the Namboku Line at Station T06.

Next we investigate the effect of our homogenization re-scheduling method. We suppose that the number of passengers waiting at G03 on the Ginza Line increases suddenly at $t = t_0$, so that the passenger density of the nearest upstream train A becomes 1 when it arrives at G03 at $t = t_1$. We have compared the evolution of the passenger density on train A in three systems: the system without re-scheduling, the system with conventional re-scheduling, and the system with homogenization re-scheduling. In Fig. 18, it can be seen that systems with re-scheduling decrease the passenger density of the train when the train is between G13 and G18. Moreover, we have found that our homogenization method is better than the conventional re-scheduling method.

5. Concluding discussions

In this chapter, we have proposed a new mathematical model for passenger transport systems, the so-called *public conveyance model*, built on the stochastic cellular automaton, which is exactly solved in the steady state. First, we defined the jamming state as a mathematical science and introduce the fundamental diagram to discuss the flow of particles. As two examples of analytical rule-based models, ASEP and ZRP, the fundamental diagrams obtained from numerical simulations and analytical calculations have been demonstrated.

As a one-dimensional case of public conveyance model, we investigated the bus route system and its efficiency by introducing three measurements: average velocity, the number of waiting passengers and transportation volume. Moreover, the effectiveness of an information-based control system, in which the number of particles between successive stops is adjusted, was discussed by comparing the case without control and with control in terms of these three measurements. As we found that implementation of the information-based traffic control system does not necessarily always improve the efficiency of the public conveyance system.

As an application of the public conveyance model, we have proposed a network simulator "KUTTY", which is based on the route choice behaviors of passengers. "KUTTY" takes into account the complex topology of the Tokyo Metro Railway Network and the OD demand estimated from the rider-ship data provided by the Tokyo Metro company. "KUTTY" can

immediately provide an estimation of the passenger flow pattern required when an accident occurs in the Tokyo Metro Railway Network. Furthermore, we have also presented a homogenization re-scheduling method to alleviate congestion of a crowded train. It is based on the idea that the number of passengers in each train should be homogeneously-distributed. We found that our method is more efficient than the conventional approach.

Finally, we hope that this mathematical model and this simulator as an application of the mathematical model can be applied to other transportation systems and help in demonstrating the dynamical patterns and estimating the efficiency, traffic volume, and the other measurements to optimize their operation.

6. Acknowledgements

This chapter is owed to colaborated works with my colleagues. I would like to give a huge thanks to Debashish Chowdhury, Andreas Schadschneider, Katsuhiro Nishinari, Rui Jiang, Daichi Yanagisawa, Ryosuke Nishi, Mitsuhito Komatsu, Il Yun Yoo, Makoto Uchida, and Ryo Takayama for enjoyable collaborations.

7. References

[1] D. Chowdhury, L. Santen and A. Schadschneider, Phys. Rep. 329 (2000), 199-329.
[2] D. Helbing, Rev. Mod. Phys. 73 (2001), 1067-1141.
[3] A. Schadschneider, D. Chowdhury and K. Nishinari, "STOCHASTIC TRANSPORT IN COMPLEX SYSTEMS FROM MOLECULES TO VEHICLES", Elsevier, (2010).
[4] K. Nishinari, “Distributed Autonomous Robotic Systems 8”, p.175 (2009).
[5] K. Nishinari, Y. Suma, D. Yanagisawa, A. Tomoeda, A. Kimura and R. Nishi, “Pedestrian and Evacuation Dynamics 2008”, pp.293-308 (2010).
[6] B Derrida, M R Evans, V Hakim and V Pasquier, J. Phys. A: Math. Gen. 26 1493 (1993).
[7] M. Schreckenberg, A. Schadschneider, K. Nagel and N. Ito, Phys. Rev. E 51 2939 (1995).
[8] F. Spitzer, Adv. Math. 5, 246 (1970).
[9] M. R. Evans, J. Phys. A: Math. Gen. 30, 5669 (1997).
[10] M. R. Evans and T. Hanney, J. Phys. A: Math. Gen. 38, R195 (2005).
[11] M. Kanai, J. Phys. A: Math. Gen. 40 pp.7127-7138 (2007).
[12] A. Tomoeda, D. Chowdhury, A. Schadschneider and K. Nishinari, Physica A, 384, 600-612 (2007).
[13] A. Tomoeda, M. Komatsu, I. Y. Yoo, M. Uchida, R. Takayama and K. Nishinari, Cellular Automata (Lecture Notes in Computer Science, Springer), 5191 (2008), 433.
[14] A. Tomoeda, M. Komatsu, I. Y. Yoo, M. Uchida, R. Takayama, R. Jiang and K. Nishinari, GESTS International Transaction on Computer Science and Engineering, 54, 81, (2009).
[15] C. Arita, Phys. Rev. E, 80, 051119, (2009).
[16] C. Arita and D. Yanagisawa, J. Stat. Phys., 141, 829, (2010).
[17] S. Wolfram, *Theory and Applications of Cellular Automata* (1986) (Singapore: World Scientific).
[18] S. Wolfram, *Cellular Automata and Complexity* (1994) (Reading, MA: Addison-Wesley).
[19] A. Schadschneider, Physica A 313, 153 (2002).
[20] R. Jiang, B. Jia and Q.S. Wu, J. Phys. A 37, 2063 (2004).
[21] O. J. O’Loan, M. R. Evans, M. E. Cates, Europhys. Lett. 42, 137 (1998); Phys. Rev. E 58, 1404 (1998).

[22] D. Chowdhury, et al., J. Phys. A, 35, L573 (2002).
[23] A. Kunwar, et al., J. Phys. Soc. Jpn., 73, 2979 (2004).
[24] A. Tomoeda and K. Nishinari, in the proceedings of "SICE Annual Conference, 2008" (2008) 549.
[25] K. Nishinari and D. Takahashi, J. Phys. A: Math. Gen. 32, 93 (1999).
[26] S. Yukawa, M. Kikuchi and S. Tadaki, J. Phys. Soc. Japan 63, 3609 (1994).
[27] M. Pursula, Simulation of traffic systems - an overview, Journal of Geographic Information and Decision Analysis 3 (1999) 1.
[28] V. Latora and M. Marchiori, Physica A, 314 (2002) 109.
[29] D. J. Watts and S.H. Strogatz, Nature, 393 (1998) 440.
[30] D. Meignan, O. Simonin and A. Koukam, Simulation Modeling Practice and Theory, 15 (2007) 659.
[31] E. W. Dijkstra, Numerische Mathematik, 1 (1959), 269.

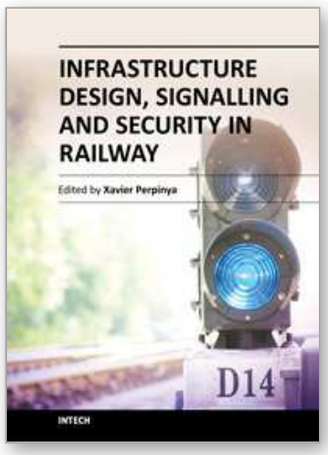

Infrastructure Design, Signalling and Security in Railway

Edited by Dr. Xavier Perpinya

ISBN 978-953-51-0448-3
Hard cover, 522 pages
Publisher InTech
Published online 04, April, 2012
Published in print edition April, 2012

Railway transportation has become one of the main technological advances of our society. Since the first railway used to carry coal from a mine in Shropshire (England, 1600), a lot of efforts have been made to improve this transportation concept. One of its milestones was the invention and development of the steam locomotive, but commercial rail travels became practical two hundred years later. From these first attempts, railway infrastructures, signalling and security have evolved and become more complex than those performed in its earlier stages. This book will provide readers a comprehensive technical guide, covering these topics and presenting a brief overview of selected railway systems in the world. The objective of the book is to serve as a valuable reference for students, educators, scientists, faculty members, researchers, and engineers.

InTech Europe
University Campus STeP Ri
Slavka Krautzeka 83/A
51000 Rijeka, Croatia
Phone: +385 (51) 770 447
Fax: +385 (51) 686 166
www.intechopen.com

InTech China
Unit 405, Office Block, Hotel Equatorial Shanghai
No.65, Yan An Road (West), Shanghai, 200040, China
中国上海市延安西路65号上海国际贵都大饭店办公楼405单元
Phone: +86-21-62489820
Fax: +86-21-62489821

IntechOpen